Regulation of experimental autoimmune encephalomyelitis by TPL-2 kinase

Srividya Sriskantharajah[#][*], **Eva Gückel**[#][*], **Niki Tsakiri**[§], **Katrin Kierdorf**[¶], **Christine Brender**[*], **Abduelhakem Ben-Addi**[*], **Marc Veldhoen**[†], **Philip N. Tsichlis**[‖], **Brigitta Stockinger**[†], **Anne O'Garra**[‡], **Marco Prinz**[¶], **George Kollias**[§,††], and **Steven C. Ley**[*,††]

[*]Divisions of Immune Cell Biology, National Institute for Medical Research, London, NW7 1AA, UK

[†]Molecular Immunology, National Institute for Medical Research, London, NW7 1AA, UK

[‡]Immunoregulation, National Institute for Medical Research, London, NW7 1AA, UK

[§]Institute for Immunology, Biomedical Sciences Research Center 'Alexander Fleming', 16672 Vari, Attica, Greece

[¶]Department of Neuropathology & BIOSS Center for Biological Signaling, University of Freiburg, D-79106 Freiburg, Germany

[‖]Molecular Oncology Research Institute, Tufts Medical Center, Boston, MA 02111, USA

[#] These authors contributed equally to this work.

Abstract

TPL-2 expression is required for efficient polarization of naïve T cells to Th1 effector cells *in vitro*, and for Th1-mediated immune responses. In the present study, we investigated the potential role of TPL-2 in Th17 cells. TPL-2 was found to be dispensable for Th17 cell differentiation *in vitro*, and for the initial priming of Th17 cells in experimental autoimmune encephalomyelitis (EAE), a Th17 cell-mediated disease model for multiple sclerosis. Nevertheless, TPL-2-deficient mice were protected from EAE, which correlated with reduced immune cell infiltration, demyelination and axonal damage in the CNS. Adoptive transfer experiments demonstrated that there was no T cell-intrinsic function for TPL-2 in EAE, and that TPL-2 signaling was not required in radiation-sensitive hematopoietic cells. Rather, TPL-2 signaling in radiation-resistant stromal cells promoted the effector phase of the disease. Importantly, using a newly generated mouse strain expressing a kinase-inactive form of TPL-2, we demonstrated that stimulation of EAE was dependent on TPL-2's catalytic activity, and not its adaptor function to stabilize the associated ubiquitin-binding protein ABIN-2. Our data therefore raise the possibility that small molecule inhibitors of TPL-2 may be beneficial in multiple sclerosis therapy.

INTRODUCTION

TPL-2, also known as COT and MAP3K8, is expressed in both hematopoietic and non-hematopoietic cells, and functions as a MAP 3-kinase that activates the MAP 2-kinases MEK-1/2 (1). During innate immune responses, TPL-2 expression is required for activating ERK-1/2 MAP kinases in myeloid cells by Toll-like receptors (TLRs), as well as the receptors for TNF and IL-1β (1-4). TPL-2 is critical for the production of TNF during TLR4-induced acute inflammatory responses, and is also required for the development of TNF-induced Crohn's-like inflammatory bowel disease (2, 5). Consequently, TPL-2 is considered an attractive drug target for TNF-dependent inflammatory diseases (6).

In contrast to its positive role in inflammation driven by innate immune cells, TPL-2 can negatively regulate Th2 cell-driven inflammation. When re-challenged with ovalbumin intranasally, ovalbumin-sensitized $Map3k8^{-/-}$ mice express higher levels of immunoglobulin E, and develop more severe broncheoalveolar inflammation (7). This augmented inflammation occurs as a consequence of a default increase in Th2 effector cells, resulting from impaired Th1 differentiation of CD4$^+$ T cells in $Map3k8^{-/-}$ mice (8), possibly through the removal of IFNγ-mediated Th2 inhibition (9). However, it has not been established that TPL-2-mediated inhibition of lung inflammation in the ovalbumin lung allergy model actually results from a T cell-intrinsic signaling function. In contrast, the protective role for TPL-2 in promoting Th1 effector cell differentiation during the immune response to *Toxoplasma gondii*, a Th1 cell-inducing parasite, has been directly demonstrated to be mediated by TPL-2 signaling in T cells (8).

Th17 cells, a subset of effector CD4$^+$ T cells characterized by the production of the cytokine IL-17 (10), are important in immune responses to bacteria and fungi. In addition, aberrant Th17 cell activation is causally linked to the development of several human autoimmune diseases. In the present study, we investigated the potential requirement for TPL-2 in cytokine-induced Th17 cell differentiation *in vitro*, and also the role of TPL-2 in experimental autoimmune encephalomyelitis (EAE), in which Th17 cells have an important pathogenic role (11). EAE is an animal model for multiple sclerosis (MS), which is induced by immunization with myelin antigens, such as myelin oligodendrocyte glycoprotein (MOG) (12). We found that TPL-2 was dispensable for cytokine-induced differentiation of naïve T cells to the Th17 cell lineage *in vitro*. Furthermore, TPL-2 was not required for the initial activation and expansion of MOG-specific Th17 cells in the periphery during EAE. Generation of interferon γ (IFNγ)-producing Th1 cells, which may also play a role in EAE (11), was also independent of TPL-2 expression. Nevertheless, TPL-2 was demonstrated to regulate both the onset and severity of EAE. Cell transfer experiments established that TPL-2 regulated the effector phase of EAE in the CNS, functioning in radiation-resistant stromal cells. Importantly, using a newly generated *Map3k8* knock-in mouse strain, we also showed that the development of EAE was dependent on TPL-2 catalytic activity, whilst ruling out any potential function of TPL-2 as scaffolding protein in the disease process. Our data therefore suggest that small molecule inhibitors of TPL-2 might be beneficial therapeutically in MS, the most common inflammatory demyelinating disease of the CNS (13).

Materials and Methods

Mice

$Map3k8^{-/-}$ (2), $Tnip2^{-/-}$ (14) and $Ifnar^{-/-}$ mice were fully backcrossed to C57BL/6. $Map3k8^{-/-}Rag1^{-/-}$ and $Ifnar^{-/-}Map3k8^{-/-}$ were generated by intercrossing the appropriate single knockout mice. For the generation of $Map3k8^{D270A/D270A}$ mice a P1-derived artificial chromosome clone (519-N17), including the $Map3k8$ gene was isolated from an RPC121

P1-derived artificial chromosome library (obtained from the UK Human Genome Mapping Project Resource Centre, Hinxton) by hybridization with an 1.5-kilobase (kb) probe encompassing full-length rat *Map3k8* cDNA. A 6.6 kb *Cla*I-*Bam*HI fragment containing exon 5, which encodes D270, was isolated and subcloned into pBluescript SK+/− (Invitrogen) to create pSK-LA ('left arm'). From this plasmid, a 3.2 kb *Pst*I fragment was subcloned into pBluescript SK+/− to create pSK-LA.PstI. PCR was used to mutate the sequence encoding D270 to alanine. To facilitate screening for the mutation, a *BssS*I site was introduced next to the 3′ of the D270A mutation without altering with the coding sequence. The D270A-containing PstI fragment was subsequently reinserted into pSK-LA, to create pSK-LA.D270A and from here a 5.2 kb *Hpa*I fragment containing the mutation was cloned into a unique *Xho*I cloning site of the pLox-AP1 vector, to produce the pLox-AP1-LA (left arm). The pLox-AP1 vector contains *neo*r flanked by two *lox*P sites and the herpes simplex virus thymidine kinase gene, both driven by the PGK1 promoter. A 4.7 kb BamH*I*-Sal*I* fragment was isolated and subcloned into pBluescript SK+/− to create pSK-RA ('right arm'). From this plasmid, a 4.4 kb Hpa*I*-Bsu36*I* fragment was subcloned into pLox-AP1-LA to create the pLox-AP1-Tpl2D270A targeting vector (Supplementary Figure 4D). The vector was linearized with Not*I* and transfected into ES cells (carried out by PolyGene AG, Switzerland). C57BL/6 (CD45.2$^+$, wild type), CD45.1 C57BL/6, CD45.1 *Rag1$^{-/-}$*, *Tcra$^{-/-}$* and *μMT$^{-/-}$* mice were bred in specific pathogen-free animal facilities of the National Institute for Medical Research (London, UK) in accordance with the UK Home Office regulations. 6–10 week old male mice were used for all experiments.

Antibodies

Antibodies to TPL-2, IκBα, ERK-1, ERK-2, actin were purchased from Santa Cruz Biotechnology, whilst p-p105 (Ser933), p-p38 and p-ERK (Thr185/Tyr187) antibodies were obtained from Invitrogen. Tubulin mAb was kindly provided by Keith Gull (University of Oxford).

A number of fluorescently labelled antibodies for flow cytometry were used against: GMSCF-PE; Gr1-FITC; CD25-PE; TCRβ-PECy5; TCRγδ-PE; Streptavidin-PerCP; Streptavidin-PE were purchased from BD Pharmingen. IL-17A-APC; IFNγ-FITC; CD4-FITC, -PE; F4/80-APC, -PE; Gr1-biotinylated; CD25-APC; CD44-AF450, -FITC; CD45.2-FITC, -AF450; CD45.1-biotinylated; CD11c-PE; CD11b-PE, -biotinylated; MHCII-biotinylated were obtained from eBioscience. CD4-PerCP; CD19-Pacific Blue were purchased from BioLegend. CD4-PE/Texas Red; CD8-PE/Texas Red were obtained from Invitrogen.

Induction and assessment of EAE

Active EAE was induced by immunizing subcutaneously with 250μg of MOG$_{35-55}$ peptide (Cambridge Research Biochemicals), emulsified in complete Freund's adjuvant (CFA), containing 250μg heat-killed *Mycobacterium tuberculosis* (H37RA; Difco Laboratories). Mice received 200ng pertussis toxin (Calbiochem) intraperitoneally on day 0 and 2 days post-immunization. For passive EAE experiments, *Map3k8$^{-/-}$* or WT mice were injected intravenously with 30×10^6 Th17-polarized MOG$_{35-55}$ specific T cells and intraperitoneally with Pertussis toxin (day 0 and 2). To generate Th17 cell populations, drain lymph node cells from *Map3k8$^{-/-}$* or WT mice were collected 10 days after immunization with MOG$_{35-55}$ peptide plus CFA. Cells were cultured for 3 days (5×10^6 cells/ml; 24-well-plates) in Iscove's modified Dulbecco medium (Sigma) supplemented with 10 % (vol/vol) heat-inactivated FCS (Labtech), 5mM L-glutamine, 50μM β-mercaptoethanol and antibiotics (all Gibco) in the presence of 10μg/ml MOG$_{35-55}$ peptide under Th17-polarizing conditions: 20ng/ml rmIL-23 (R&D) plus 20ng/ml rmIL-1β (Invitrogen), or Th1-polarizing conditions: 20ng/ml rmIL-12 (R&D) and 1μg/ml αIL-23p19 (eBioscience). Clinical signs of disease

were assigned daily: 0, no symptoms of disease; 1, loss of tail tonicity; 2, hind limb weakness/impaired gait; 3, partial hind limb paralysis; 4, complete hind limb paralysis; 5, forelimb paralysis or moribund.

Generation of bone marrow radiation chimeras

Bone marrow cells from $Map3k8^{-/-}$ or WT control mice were depleted of T cells with biotinylated TCRβ mAb (H57-597: BD Phamingen) and streptavidin-labelled magnetic beads (Dynal, Invitrogen). $5 - 10 \times 10^6$ cells were then transferred by intravenous injection into lethally irradiated (twice 400 rads) $Rag1^{-/-}$ or $Tpl2^{-/-}$ $Rag1^{-/-}$ hosts. For mixed bone marrow chimeras, WT or $Map3k8^{-/-}$ bone marrow cells were mixed with $Tcra^{-/-}$ or $\mu MT^{-/-}$ bone marrow cells at a ratio of 1:4, prior to injection into sub-lethally irradiated (500 rads) $Rag1^{-/-}$ mice. EAE was induced 6-8 weeks after cell transfer.

Isolation of CNS cells

Brains and spinal cords were mechanically homogenized and passed through a 70μm cell strainer (BD Pharmingen). Cells were centrifuged at $400 \times g$ for 5 min at 4°C, and lymphocytes separated on a 36.5% Percoll gradient (GE Healthcare) prior to flow cytometric staining.

Histological analysis

Spinal cords were removed and fixed in 4% formalin. Paraffin embedded sections were stained, as previously described (15), with luxol fast blue (LFB), anti-CD3 (Serotec), anti-Mac-3, anti-B220 (both BD Pharmingen) and amyloid precursor protein (APP) (Chemicon).

T cell recall assay

Lymph node cells were isolated from mice 9 days after immunization with MOG_{35-55} peptide. Cells were cultured for 24 h in complete medium (2×10^6 cells/ml; 96-well-flat-bottomed plates) containing 10μg/ml MOG_{35-55} peptide, and supernatants collected for quantification of IL-17 and IFNγ by ELISA. For proliferation assays, lymph node cells were labelled with carboxyfluorescein succinimidyl ester (CFSE; Molecular Probes) as described previously (16), and cultured for a total of 72h.

ELISA quantitation of cytokines

Levels of IL-17 and IFNγ were quantified by ELISA according to the manufacturer's protocol (eBioscience).

Real-time quantitative PCR

Spinal cord tissue was collected in RNA*later* stabilisation buffer (Qiagen) 15 days after MOG_{35-55} peptide/CFA immunization. Total RNA was isolated from spinal cords, cultured T cells, and primary cultures of microglia and astrocytes (RNeasy kit, Qiagen). After treatment with DNAase I (Invitrogen), cDNA was synthesised (1μg RNA; SuperScript First Strand Synthesis System, Invitrogen), and expression of mRNA determined using an Applied Biosystems ABI Prism 7000 Sequence Detection System and commercial FAM labelled probes (Applied Biosystems). Gene expression is displayed in arbitrary units relative to *Hprt* mRNA (encoding hypoxanthine guanine phosphoribosyl transferase).

Protein Analyses

Purified BMDM, BMDC and T cells were serum-starved for 12 h (1% FCS) to reduce basal ERK activation. BMDM and BMDC were stimulated with 1μg/ml heat-inactivated *Mtb* (Difco Laboratories), while CD4$^+$ T cells were stimulated with soluble anti-CD3 (1 μg/ml;

BD Pharmingen) plus anti-CD28 (1 μg/ml; BD Pharmingen). Cultured primary microglia and astrocytes were stimulated with LPS (100 ng/ml; Enzo), murine recombinant TNF (50 ng/ml, R&D), IFNγ (100 ng/ml; R&D), IL-1β (20 ng/ml; Peprotech) and IL-17A (100 ng/ml; R&D), alone or in the indicated combinations. Cells were washed once in PBS before lysis in buffer A (50 mM Tris, pH 7.5, 150 mM NaCl, 1 mM EDTA, 1 mM EGTA, 50 mM NaF, 1 mM Na3VO4, 100 nM okadaic acid; Calbiochem, 2 mM Na4P2O7 plus protease inhibitors) containing 1% Nonidet-P40, 0.5% deoxycholate and 0.1% SDS. Centrifuged lysates were mixed with an equal volume of 2× Laemmli sample buffer, resolved by SDS-PAGE, and immunoblotted. Protein concentration in lysates was determined by Bradford assay (Bio-Rad).

Flow cytometry

Single-cell suspensions were obtained from LN, spleen, brain or spinal cords of mice via gentle homogenisation through nylon mesh filters (70μM, BD Pharmingen). Cell concentrations were determined using a Casy Counter (Scharfe Instrument Systems). Erythrocytes in spleen samples were lysed prior to staining.

For analysis of surface markers, cells were stained with the indicated antibodies in PBS (2% (wt/vol) BSA). For intracellular cytokine staining, cells were restimulated for 4 h with PdBU (0.5μg/ml; Sigma), Ionomycin (0.5μg/ml; Sigma) and Brefeldin A (1μg/ml; GolgiPlug; BD Pharmingen), or with MOG$_{35-55}$ peptide for 12 h, adding Brefeldin A for the last 4 h of culture. Cells were stained for surface antigens as indicated, fixed for 15 min in 4 % (vol/vol) paraformaldehyde (Sigma) and permeabilized with 0.1 % (vol/vol) Nonidet-P40 for 4 min. Intracellular antibodies were added in PBS containing 0.01% (vol/vol) sodium azide and 24G2 cell supernatant to block Fc receptor binding. Four- and seven-colour cytometric staining was analyzed on FACSCalibur and Cyan instruments (Becton Dickinson), respectively. Data analysis was performed with FlowJo V8.5 software (TreeStar).

Cell culture and purification

Macrophages and myeloid DC were generated from BM stem cells as described previously (17), with purities of 95% for BMDM (F4/80^{+}) and BMDC (CD11c^{+}) cell populations. For biochemical analyses, CD4^{+} T cells were purified (95% CD4^{+}) from single-cell suspensions prepared from LN by negative selection as described (16). For the isolation of naïve T cells, CD4^{+} T cells were prepared from pooled lymph nodes and spleens by negative selection, as described above. Cells were then stained with anti-CD4 (RM45, BD Biosciences), anti-CD25 (PC61.5; eBioscience) and anti-CD44 (IM7; BD Biosciences), and CD4^{+}CD44^{lo}CD25^{−} naïve cells isolated to purities of over 98% on a MoFlo cytometer (Dako Cytomation). Naïve T cells were differentiated into Th17 cells as described (18, 19).

Mixed glial cultures were prepared from 1-2 day old mice using a published protocol (20). In brief, brains were dissected and meninges were removed. Brains were mechanically homogenized and passed through a 70μm cell strainer (BD Pharmingen). The resulting cell suspension was cultured in DMEM (Invitrogen) supplemented with 10% heat-inactivated FCS, antibiotics and 20% L929 cell supernatant, with medium changes every 3-4 days. After 10 – 14 days, the floating and loosely adherent microglial cells were harvested by vigorous shaking of culture flasks (250 r.p.m., 3h, 37 °C), before being re-plated at 2.0×10^5 in 24-well-plates and stimulated the following day. Adherent astrocytes were trypsinized, seeded at densities of 1.0×10^6 per 6-well, rested overnight in 1% serum and stimulated the following day. Microglial cell populations were 98 % CD11b^{+}, while astrocyte cell populations were 85% GFAP^{+} (glial fibrillary acidic protein-staining), as determined by flow cytometry.

Statistics

Data are presented as means ± s.e.m. For analysis of clinical scores, a two-way analysis of variance (ANOVA) with Bonferroni correction was applied. An unpaired Student's t-test with 2-tailed p-values was used for statistical analysis of *in vitro* assays. A non-parametric Mann-Whitney U-test was used for statistical analyses of flow cytometric data. All statistical analyses were calculated using Graph Pad Prism 5 software. P-values of less than 0.05 were considered significant.

Results

TPL-2 is not essential for *in vitro* generation of Th17 polarized cells

TPL-2 is required for efficient polarization of naïve CD4$^+$ T cells to interferon γ (IFNγ)-producing Th1 cells *in vitro*, and *in vivo* after *T. gondii* infection (8). To initially determine whether TPL-2 was required for polarization to the Th17 cell lineage, CD25$^-$ CD44^{lo} CD4$^+$ T cells from wild type (WT) and *Map3k8*$^{-/-}$ mice were cultured under Th17-polarizing conditions (19). Intracellular staining revealed that TPL-2 deficiency did not significantly reduce the fraction of IL-17A$^+$ cells (Fig. 1A and B). The amount of IL-17A in culture supernatants was also equivalent between WT and *Map3k8*$^{-/-}$ cells (Fig. 1C). Similarly, TPL-2 expression was not required for production of IL-17A$^+$ cells or IL-17 protein in culture supernatants when either IL-1β or the Aryl Hydrocarbon Receptor (AhR) ligand 6-formylindolo[3,2-b]carbazole (FICZ) (18, 21) were added to the culture medium (Fig. 1A – D).

Quantitative real-time PCR was used to determine whether TPL-2 regulated the induction of other Th17 signature cytokines and transcription factors (22). Steady-state levels of *Il17a, Il17f and Il21* mRNAs were equivalent in *Map3k8*$^{-/-}$ and WT CD4$^+$ T cells, in each of the conditions tested (Fig. 1D). The abundance of *Il22* mRNA in IL-1β or FICZ containing cultures was also similar between *Map3k8*$^{-/-}$ and WT CD4$^+$ cell cultures (18). The orphan nuclear receptor ROR-γt, which is selectively expressed in Th17 cells, induces the development of Th17 cells, in conjunction with ROR-α (23, 24). Expression of mRNAs encoding ROR-γt and ROR-α was comparable in *Map3k8*$^{-/-}$ and WT CD4$^+$ T cells (Fig. 1D). TPL-2, therefore, was not essential for *in vitro* differentiation of CD4$^+$ T cells to the Th17 cell lineage.

TPL-2 regulates the onset and severity of EAE

To investigate the physiological role of TPL-2 in Th17 cell development and function, we tested the susceptibility of *Map3k8*$^{-/-}$ mice to EAE, a Th17 cell-mediated animal model for multiple sclerosis (11). *Map3k8*$^{-/-}$ mice and control C57BL/6 WT mice were immunized with MOG$_{35-55}$, and disease progression monitored (13). Despite 100% incidence, *Map3k8*$^{-/-}$ mice showed a delay in the onset and a reduced disease severity relative to controls (Fig. 2A and Table 1). Accordingly, flow cytometric analyses at the peak of disease revealed significantly fewer CD45$^+$ hematopoietic cells, including CD4$^+$ and CD8$^+$ T cells, CD19$^+$ B cells, dendritic cells (DC), CD45$^+$CD11b$^+$ macrophages and neutrophils, in the spinal cords of *Map3k8*$^{-/-}$ mice compared to WT mice (Fig. 2B).

Intracellular staining showed similar proportions of CD4$^+$ T cells expressing IFNγ and GM-CSF in the spinal cord between WT and *Map3k8*$^{-/-}$ mice (Fig. 2C, upper panel). However, the fraction of CD4$^+$ cells producing IL-17A was significantly decreased by approximately 50% in the absence of TPL-2. Consistent with the overall decrease in CD4$^+$ T cell number, the total numbers of CD4$^+$ T cells expressing each of these encephalitogenic cytokines were significantly reduced in *Map3k8*$^{-/-}$ mice (Fig. 2C, lower panel). The proportions of γδT cells expressing IL-17A and IFNγ in the CNS were unaffected by TPL-2 deficiency, and

total γδT cell numbers were not statistically significantly different from WT (Supplemental Fig. 1A). Immunohistochemistry confirmed reduced infiltration of T and B cells, and macrophages in the spinal cords of *Map3k8*^{−/−} mice, accompanied by significantly reduced degrees of demyelination and neuronal damage (Fig. 2D and E).

A number of pro-inflammatory cytokines and chemokines are produced in the spinal cord by infiltrating reactivated CD4^{+} T cells, and activated CNS-resident cells (25, 26). Quantitative RT-PCR demonstrated significantly reduced amounts of mRNAs encoding the majority of these proteins in the spinal cords of *Map3k8*^{−/−}mice at the peak of disease (Supplemental Fig. 1B). In contrast, steady-state levels of *Il12a* and *Il12b* mRNAs were increased, consistent with earlier *in vitro* studies (27).

Together these data indicate that TPL-2 deficiency protected mice from EAE by limiting CNS inflammation, thereby reducing demyelination and axonal damage.

TPL-2 is not required for T cell priming during EAE

The disease course of EAE can be considered to occur in two stages: a priming phase, in which immunization leads to activation and expansion of peripheral myelin-specific T cells, and an effector phase in which infiltrating inflammatory cells cause CNS damage. The priming phase involves the stimulation and expansion of myelin-responsive T cells by activated antigen-presenting DC in lymph nodes. The production of IL-1β, IL-6 and IL-23 by DC, and other innate immune cells, is critical for the initial induction of Th17 cells during an immune response (10), and signaling via each of these cytokines is essential for EAE induction (21, 25). Since TPL-2 has an established signaling function in DC, we initially investigated the effect of TPL-2 deficiency on the induction of Th17 polarizing cytokines by bone marrow-derived DC (BMDC) in response to heat-inactivated *Mycobacterium tuberculosis* (*Mtb*[HI]).

Immunoblotting of cell lysates revealed that TPL-2 deficiency blocked the early activation of ERK by *Mtb*[HI], while a second wave of ERK-1/2 phosphorylation was TPL-2-independent (Supplemental Fig. 2A). p38 activation was also reduced in *Map3k8*^{−/−} BMDC, similar to the reported effects of TPL-2 deficiency after LPS stimulation (27). Despite these decreases in MAP kinase activation, qRT-PCR revealed that *Mtb*[HI] was still able to induce *Il6* and *Il23p19* mRNAs to similar levels in *Map3k8*^{−/−} and WT BMDC (Supplemental Fig. 2B). TPL-2 deficiency reduced the induction of *Il1b* mRNA by approximately 40%, while the induction of *Il12b* mRNA was increased. TPL-2 deficiency had similar effects on *Mtb*[HI] induction of ERK-1/2 activation and cytokines expression in BM-derived macrophages (BMDM) (Supplemental Fig. 3A and B). These data indicated that TPL-2 was not essential for the induction of Th17 polarizing cytokines by *Mtb*[HI] in BMDC and BMDM, although *Mtb*[HI] activation of ERK was largely dependent on TPL-2-expression in both cell types. Consistently, *Map3k8*^{−/−} BMDC were able to induce IL-17A production by CD4^{+} T cells to the same extent as WT BMDC in an *in vitro* Th17 differentiation assay (Supplemental Fig. 2C and D) (19).

Our *in vitro* experiments suggested that TPL-2 expressed in antigen-presenting DC and in responding CD4^{+} T cells might not be essential for initial generation of Th17 cells in EAE. To investigate this, the *in vivo* priming and differentiation of Th17 cells was examined in WT and *Map3k8*^{−/−} mice during the early stages of EAE. Analysis of draining lymph nodes (dLN) isolated from mice nine days after MOG$_{35-55}$ immunization revealed that both the total cellularity and CD4^{+} T cell numbers were unaffected by TPL-2 deficiency (Fig. 3A). This suggested that the activation and expansion of MOG$_{35-55}$-specific *Map3k8*^{−/−} CD4^{+} T cells occurred normally. To quantify the antigen-specific T cell response, dLN cells were labeled with carboxyfluoresceine diacetate succinimidyl ester (CFSE) and restimulated *in*

vitro with MOG$_{35-55}$. Consistent with normal priming in EAE, a similar fraction of MOG$_{35-55}$-specific CD4$^+$ T cells divided within the WT and *Map3k8$^{-/-}$* LN cell populations (Fig. 3B).

Although T cell activation and expansion in EAE were unaffected by TPL-2 deficiency, it was possible that the ability of responding T cells to differentiate into Th17 and/or Th1 cells following MOG$_{35-55}$ immunization was impaired. However, restimulation of dLN cells with either MOG$_{35-55}$ peptide or PdBU and ionomycin revealed a similar fraction of IFNγ- and IL-17A-producing CD4$^+$ T cells, as well as a similar production of both cytokines by MOG$_{35-55}$-specific CD4$^+$ T cells from immunized WT and *Map3k8$^{-/-}$* mice (Fig. 3C and D).

In vivo experiments therefore indicated that CD4$^+$ T cell activation, expansion and differentiation into Th1 and Th17 effector cells occurred independently of TPL-2. These results were consistent with the ability of *Map3k8$^{-/-}$* CD4$^+$ T cells to activate ERK-1/2 (Supplemental Fig. 3C) and proliferate normally in response to CD3/CD28 crosslinking (16), and for *Map3k8$^{-/-}$* BMDC to induce differentiation of CD4$^+$ T cells to the Th17 cell lineage *in vitro* to a similar extent as WT BMDC (Supplemental Fig. 2C).

TPL-2 does not function within T cells to promote EAE

Defective T cell priming did not explain the reduced susceptibility of *Map3k8$^{-/-}$* mice to EAE. Nevertheless, it remained possible that TPL-2 had a T cell-intrinsic function at a later stage in EAE pathogenesis. This was investigated by mixing BM cells from *Tcra$^{-/-}$* mice with WT or *Map3k8$^{-/-}$* BM cells (ratio 4:1), before transferring them into *Rag1$^{-/-}$* hosts. In the resulting chimeras, all of the T cells developed from either WT or TPL-2-deficient donor BM, whilst the majority (80%) of the other hematopoetic cells was derived from the TPL-2-sufficient *Tcra$^{-/-}$* BM. Upon induction, the onset and severity of EAE were essentially identical in both sets of mixed BM chimeras (Fig. 4A), indicating that there was no T cell-intrinsic function for TPL-2 in EAE pathogenesis.

The potential function of TPL-2 in T cells was also investigated in a passive EAE model, in which encephalitogenic myelin-responsive T cells were transferred into naïve recipients (13). Draining LN cells were isolated from *Map3k8$^{-/-}$* mice nine days after MOG$_{35-55}$ immunization, and then cultured with MOG$_{35-55}$ peptide, IL-1β and IL-23 to expand MOG$_{35-55}$-specific Th17 cells (28). Intracellular cytokine staining indicated similar polarization efficiency within WT and *Map3k8$^{-/-}$* CD4$^+$ T cell populations (data not shown). Following intravenous injection, the onset and extent of EAE induced by transferred *Map3k8$^{-/-}$* and WT Th17-polarized cells were very similar (Fig. 4B), consistent with the results of active EAE in mixed BM chimeras.

CD20 antibody depletion has demonstrated that B cells promote EAE disease progression via production of IL-6 (29, 30), in addition to their late-acting regulatory role (31, 32). TPL-2 is known to regulate ERK-1/2 activation in B cells following CD40 and TLR stimulation (3, 33), raising the possibility that the protection of *Map3k8$^{-/-}$* mice from EAE might be due to TPL-2 signaling in B cells. To investigate this, chimeric mice were generated in which BM from *μMT$^{-/-}$* mice was mixed with *Map3k8$^{-/-}$* BM cells (ratio 4:1), and injected into lethally irradiated *Rag1$^{-/-}$* recipients. The onset and severity of EAE were similar between mice lacking TPL-2 expression in B cells and WT controls (Supplemental Fig. 4A). Therefore, the protection from EAE observed in *Map3k8$^{-/-}$* mice was not due to the absence of TPL-2 in T or B cells.

TPL-2 signaling in radiation-resistant cells promotes the effector phase of EAE

Since the priming phase of EAE was normal in *Map3k8*−/− mice, this suggested that TPL-2 functioned during the effector phase of the disease. To investigate this, the ability of WT MOG$_{35\text{-}55}$ peptide-primed Th17 cells to induce passive EAE in WT and *Map3k8*−/− recipient mice was determined. A delay in onset of clinical symptoms and a reduction in disease severity were observed upon transfer of encephalitogenic Th17-polarized cells into *Map3k8*−/− mice (Fig. 4B). TPL-2-deficient mice were also protected from EAE induced by WT MOG$_{35\text{-}55}$ peptide-primed Th1 cells, suggesting the protection from disease did not involve a Th-cell specific factor (Supplemental Fig. 4B and C).

The effector phase of EAE involves two waves of immune cell infiltration into the CNS (34-36). Firstly, 'pioneer' MOG$_{35\text{-}55}$-specific CD4$^+$ T cells enter the brain via the choroid plexus. Inflammatory cytokines produced by re-activated CD4$^+$ T cells then induce recruitment of a second wave of infiltrating immune cells. We investigated the recruitment of immune cells to the CNS in passive EAE. CD45.1$^+$ MOG$_{35\text{-}55}$ peptide-primed Th17 cells generated from WT mice were transferred to CD45.2$^+$ WT or *Map3k8*−/− mice. Similar numbers of CD45.1$^+$ CD4$^+$ T cells were detected in the spleens and brains of WT and *Map3k8*−/− mice early after adoptive transfer (Fig. 5A, left and middle panels). However, at the peak of the disease, significantly more CD45.1$^+$ CD4$^+$ T cells accumulated in the brains of WT relative to *Map3k8*−/− mice (Fig. 5A, middle panel). Moreover, consistent with a defect in secondary immune cell infiltration into *Map3k8*−/− brains, fewer CD45$^+$F4/80$^+$ macrophages were detected 14 days after Th17 cell transfer (Fig. 5A, right panel). The number of CD45.1$^+$ CD4$^+$ T cells in the spleen at these later time points was similar between the two recipient CD45.2$^+$ genotypes, demonstrating that host TPL-2 expression was not required for CD4$^+$ T cell survival (Fig. 5A, left panel). Furthermore, transferred CD4$^+$ T cells in the CNS of *Map3k8*−/− hosts produced similar fractions of IFNγ and IL-17 to WT hosts (Fig. 5B). 'Pioneer' Th17 cells, therefore, could infiltrate the CNS of *Map3k8*−/− mice, but failed to optimally trigger a secondary infiltration of immune cells, the major mediators of myelin damage.

Although transfer of encephalitogenic Th17 cells demonstrated that the TPL-2 deficient host environment was protective in passive EAE (Fig. 4B), it did not reveal whether TPL-2 promoted EAE by signaling in hematopoietic cells other than T or B cells. This was investigated by generating BM chimeras, via transferring WT or *Map3k8*−/− BM cells into lethally irradiated *Rag1*−/− or *Rag1*−/−*Map3k8*−/− recipients. In these chimeras, all lymphocytes, and more than 99% of MHC Class II$^+$ cells, were of donor-origin (data not shown). Upon EAE induction, deletion of TPL-2 in radiation-sensitive cells (*Map3k8*−/− > *Rag1*−/− compared with *Map3k8*+/+ > *Rag1*−/−) was not able to protect against disease (Fig. 6A). However, transferring WT BM cells into *Rag1*−/− hosts that additionally lacked TPL-2 resulted in delayed EAE onset. Furthermore, lack of TPL-2 expression in the radiation-resistant compartment resulted in a reduction in immune infiltrates in the spinal cord (Fig. 6B), but did not affect polarization of CD4$^+$ T cells to produce IL-17A and IFNγ (Fig. 6C). Therefore, TPL-2 promoted the effector phase of EAE by signaling in radiation-resistant non-hematopoietic cells, which induced the secondary infiltration of immune cells into the CNS parenchyma.

TPL-2 signals in both microglia and astrocytes

CNS-resident microglia and astrocytes have been reported previously to play pivotal roles in EAE disease manifestation (20, 37, 38). These radiation-resistant cell types produce a number of pro-inflammatory cytokines and chemokines during EAE, which promote the secondary influx of hematopoietic cells into the CNS (34, 36, 39). Defective activation of one or both of these cell types, therefore, could account for the protection of *Map3k8*−/−

mice from EAE development. We explored this possibility by determining whether TPL-2 deficiency affected cytokine and chemokine induction in primary *in vitro*-derived microglia and astrocytes.

Map3k8$^{-/-}$ microglia expressed significantly less *Il6, Il1, Cxcl1, Ccl2* and *Ccl20* mRNAs in response to LPS stimulation than their WT counterparts (Fig. 7A). In addition, induction of *Il1* and *Ccl2* mRNAs was reduced by TPL-2 deficiency following stimulation with IFNγ, or TNF plus IFNγ (Fig. 7 A and B). LPS upregulation of mRNAs encoding IL-6, IL-1β, CCL2, CXCL1, VCAM1 and MMP9 was also significantly reduced in *Map3k8*$^{-/-}$ astrocytes compared to WT control cells (Fig. 7C). Furthermore, IL-1β induction of *Il6, Ccl2* and *Vcam1* mRNAs, as well as TNF induction of *Ccl2* and *Mmp9* mRNAs, were reduced by TPL-2 deficiency in astrocytes (Fig. 7C). Defective TNF induction of *Ccl2, Vcam1* and *Mmp9* mRNAs in *Map3k8*$^{-/-}$ astrocytes was not rescued by co-stimulation with IL-17A (Fig. 7D). In line with earlier studies, stimulation of astrocytes with IL-17A alone had minimal effect on the expression of mRNAs encoding pro-inflammatory cytokines or chemokines in astrocytes (20, 40).

We next analysed the activation of MAP kinase signaling pathways in microglia and astrocytes to gain insight into how TPL-2 deficiency might impair pro-inflammatory gene expression in these cell types. In line with earlier studies using primary macrophages and dendritic cells (2, 3, 27), ERK-1/2 and p38α phosphorylation following LPS or TNF stimulation of microglia was reduced by TPL-2 deficiency (Fig. 8A). Analysis of NF-κB1 p105 phosphorylation (data not shown) indicated that this decrease did not result from impaired activation of the IKK complex (41). Phosphorylation of ERK-1/2 and p38α was not induced by stimulation with either IFNγ or IL-17A (data not shown).

ERK-1 and 2 were basally phosphorylated at high levels in astrocytes, and this was not detectably altered by stimulation with LPS or TNF (Fig. 8B). However, LPS and TNF clearly induced p38α phosphorylation, and this was partially decreased by TPL-2 deficiency following stimulation with either agonist. Addition of IFNγ or IL-17A did not alter p38α phosphorylation in astrocytes (data not shown).

In conclusion, our biochemical analyses demonstrated that TPL-2 contributed to p38α activation in both microglia and astrocytes after stimulation with LPS and TNF, and was also required for optimal activation of ERK-1/2 in microglia by these agonists. Together with the qRT-PCR analyses of cytokine and chemokine mRNA expression (Fig. 7), these data were consistent with the hypothesis that TPL-2 signaling in both microglia and astrocytes could contribute to EAE disease development.

TPL-2 kinase activity is required for development of EAE

TPL-2 is associated with the ubiquitin-binding protein ABIN-2, which is required to maintain TPL-2 stability (42). ABIN-2-deficient mice have reduced steady-state levels of TPL-2 in multiple cell type compared to WT mice (14). In a reciprocal fashion, analysis of cells from *Map3k8*$^{-/-}$ mice revealed that TPL-2 is required to maintain steady-state expression of ABIN-2, and both splenocytes and BMDM from *Map3k8*$^{-/-}$ mice have substantially reduced amounts of ABIN-2 compared to WT (Fig. 9A). This suggested that the resistance of *Map3k8*$^{-/-}$ mice to EAE might result from reduced ABIN-2 expression. However, EAE disease severity was similar between *Tnip2*$^{-/-}$ (which completely lack ABIN-2 expression) and WT mice (Fig. 9B). These data indicated ABIN-2 was not required for EAE development, and suggested that the low levels of TPL-2 expressed in *Tnip2*$^{-/-}$ mice were sufficient to promote maximal disease.

Together our analyses of *Map3k8*^{−/−} and *Tnip2*^{−/−} mice demonstrated that TPL-2 expression was required for efficient EAE development. However, these experiments did not establish whether this reflected a role for TPL-2 catalytic activity, and it remained possible that TPL-2 promoted disease by functioning as an adaptor protein. To distinguish these possibilities, we generated a novel knock-in mouse strain expressing mutant TPL-2[D270A] (Supplemental Fig. 4D), which is catalytically inactive (43). In contrast to *Map3k8*^{−/−} cells, *Map3k8*[D270A/D270A] cells expressed similar amounts of ABIN-2 as WT cells (Fig. 7A). Compared to WT controls, EAE development was delayed and reduced in severity in *Map3k8*[D270A/D270A] mice (Fig. 9C), similar to *Map3k8*^{−/−} mice. TPL-2 catalytic activity was therefore required to promote EAE, and this was independent of effects on the steady-state expression of ABIN-2 protein, or any potential adaptor function of TPL-2.

TPL-2 promotes EAE independently of type I interferon signaling

Development of EAE is exacerbated in mice deficient in type I interferon receptor (IFNAR), with markedly higher inflammation and demyelination in the CNS compared to WT controls (44). TPL-2/ERK-1/2 signaling negatively regulates TLR induction of IFN-β (27), raising the possibility that TPL-2 deficiency might reduce EAE disease severity by augmenting IFN-β production. We investigated this possibility genetically by generating *Map3k8*^{−/−} *Ifnar*^{−/−} mice, lacking expression of both TPL-2 and the receptor for type I IFNs, IFNAR.

As reported previously (44), IFNAR-deficiency did not affect EAE disease onset, but increased the severity and duration of the effector phase (Fig. 9D). However, the onset of EAE and maximal clinical scores were similar in *Map3k8*^{−/−} and *Map3k8*^{−/−} *Ifnar*^{−/−} mice. The inhibitory effects of TPL-2 deficiency on EAE development, therefore, were independent of type I IFN signaling.

Discussion

We investigated the potential role of the MAP 3-kinase TPL-2 in Th17 cell generation and function. Our results show that TPL-2 was dispensable for the generation of Th17 cells *in vitro*, and during the priming phase of EAE. Nevertheless, TPL-2 regulated both the onset and severity of EAE, functioning in the effector phase of this Th17 cell-mediated autoimmune disease model. Importantly, the effects of TPL-2 in EAE required its catalytic activity, suggesting that small molecule inhibitors of TPL-2 might be therapeutically beneficial in multiple sclerosis (MS). IFN-β is widely used for treatment of relapsing-remitting MS (45). TPL-2 promoted EAE independently of type I IFN signaling, raising the possibility that administration of a TPL-2 inhibitor in combination with the established drug IFN-β might be more effective for MS therapy.

Earlier pharmacological studies with the MEK-1/2 inhibitor U0126 have suggested that ERK-1/2 activation is required for induction of the Th17 polarizing cytokines IL-1β and IL-23 in DC following stimulation with *Mtb*[HI] (28). *Mtb*[HI] can potentially activate multiple pattern recognition receptors on DC, including TLR-2, TLR-4, TLR-9, NOD-2 and C-type lectins (46, 47). TPL-2 is required for activation of ERK-1/2 in DC following TLR2, TLR4 or TLR9 stimulation (4, 27), and also contributes to the activation of ERK in macrophages following NOD-1 and NOD-2 stimulation, but is dispensable for activation of ERK-1/2 by the C-type lectin Dectin-1 (4). Consistent with this, stimulation of ERK phosphorylation by *Mtb*[HI] was largely dependent on TPL-2 expression in BMDC. However, TPL-2 deficiency only partially reduced *Mtb*[HI] induction of IL-1β, and did not impair induction of mRNAs encoding IL-6, IL-12p35 or IL-23p19 in these cells, which were able to induce normal Th17 cell differentiation *in vitro*. In line with these data, the generation of Th17 cells in the draining LN during the priming phase of EAE was unaffected by TPL-2 deficiency. It is

likely that low levels of TPL-2-independent ERK-1/2 activation explain the ability of $Map3k8^{-/-}$ BMDC to induce mRNAs encoding IL-1β and IL-23p19.

Experiments with lethally irradiated BM chimeras demonstrated that TPL-2 functioned in a radiation-resistant cell population to promote EAE, implying that TPL-2 signaling was not required in T cells, or antigen presenting cells (DC, macrophages). These data are consistent with *in vitro* experiments showing that TPL-2 expression was dispensable for Th17 cell differentiation induced with recombinant cytokines, or for Mtb^{HI} induction of Th17 polarizing cytokines in BMDC and BMDM. Furthermore, mixed BM chimera experiments demonstrated that TPL-2 expression in either T or B cells was not required for EAE development. Instead, passive EAE experiments using MOG_{35-55}-specific Th17 cells revealed that TPL-2 signaling in host cells regulated the effector phase of disease in the CNS. A similar requirement for host TPL-2 was found after adoptive transfer of WT MOG_{35-55} -specific Th1 cells. Therefore, TPL-2 did not have a Th17-specific function in the effector phase of EAE.

After priming in lymph nodes, antigen-specific Th17 cells traffic through the choroid plexus into the subarachnoid space, where they are reactivated (35). As a consequence of productive T cell-APC interactions, Th17 cell cytokines and chemokines are then produced, which activate parenchymal vasculature. This promotes a secondary wave of leukocyte infiltration, leading to inflammatory CNS damage and EAE onset (34). Passive EAE experiments indicated that the initial trafficking of Th17 cells into the brain was not affected by TPL-2 deficiency. Rather that TPL-2 was required for the second wave of leukocyte recruitment into the CNS. The expression of several chemokines known to be involved in regulating the migration of leukocytes into the CNS was significantly reduced in intact $Map3k8^{-/-}$ mice during EAE, including CCL2, CCL3, CCL5 and CXCL10, which have each been implicated to have positive roles in EAE induction (34). The protective effect of TPL-2 deficiency in EAE, therefore, may result from impaired upregulation of these chemokines in CNS-resident cells.

An important outstanding question is the identity of the radiation-resistant non-hematopoietic cell type in which TPL-2 signals to promote EAE. *In vitro* experiments indicated that TPL-2 was required for optimal ERK-1/2 and p38α activation in microglia, resident myeloid-lineage cells in the brain and spinal cord (48). Microglia can contribute to EAE disease initiation by presenting antigens to naïve T cells, and are also a potent source of inflammatory cytokines and chemokines (37, 39). In addition, our *in vitro* experiments revealed that TPL-2 signaling contributes to the activation of p38α in astrocytes, the most abundant cells of the brain which also produce cytokines and chemokines, and have an important role in regulating the recruitment and function of T cells in the CNS (39). TPL-2 expression was found to be required for optimal expression of pro-inflammatory cytokines and chemokines in both microglia and astrocytes, possibly due to TPL-2's contribution to MAP kinase activation in these cell types. Earlier studies with knockout mice have shown the importance of the affected cytokines and chemokines for EAE disease development (34, 39). Our data raise the possibility that the reduced secondary infiltration of inflammatory cells into the CNS in $Map3k8^{-/-}$ mice compared to WT controls during EAE results from the decreased expression of cytokines and chemokines by microglia and astrocytes.

Genetic deletion of IKK2 or NEMO in neuroectodermal-derived cells ameliorates EAE in mice, which correlates with decreased expression of proinflammatory cytokines and chemokines by CNS-resident cells (38). Recently, it has also been shown that conditional deletion of *Tak1*, which functions upsteam of the IKK complex, in either astrocytes or microglia also ameliorates EAE development (49). The IKK complex is a critical positive regulator of the TPL-2 signaling pathway, inducing proteolysis of its inhibitor NF-κB1 p105

(50, 51) and directly phosphorylating a key regulatory serine in the TPL-2 C-terminus (52). The protective effects of IKK2/NEMO deficiency in astrocytes or TAK1 deficiency in astrocytes and microglia, therefore, may be mediated in part by blockade of TPL-2 signaling. The generation of conditional knockout mouse strains lacking TPL-2 expression in astrocytes or microglia will be essential to determine whether TPL-2 signaling in either or both these cell types is important for development of EAE.

Earlier studies of *Map3k8*$^{-/-}$ mice identified TPL-2 as a potential drug target in septic shock, and inflammatory bowel disease (2, 5). Interestingly, *Mapk1* was recently identified as a disease susceptibility gene locus in multiple sclerosis (53). *Mapk1* encodes ERK2, a major downstream target of TPL-2 signaling. These data, together with the present study, suggest that blockade of TPL-2 catalytic activity might also be therapeutically beneficial in multiple sclerosis.

Supplementary Material

Refer to Web version on PubMed Central for supplementary material.

Acknowledgments

References

1. Gantke T, Sriskantharajah S, Ley SC. Regulation and function of TPL-2, an IκB kinase-regulated MAP kinase kinase kinase. Cell Res. 2010; 21:131–145. [PubMed: 21135874]

2. Dumitru CD, Ceci JD, Tsatsanis C, Kontoyiannis D, Stamatakis K, Lin J-H, Patriotis C, Jenkins NA, Copeland NG, Kollias G, Tsichlis PN. TNFα induction by LPS is regulated post-transcriptionally via a TPL2/ERK-dependent pathway. Cell. 2000; 103:1071–1083. [PubMed: 11163183]

3. Eliopoulos AG, Wang C-C, Dumitru CD, Tsichlis PN. TPL-2 transduces CD40 and TNF signals that activate ERK and regulates IgE induction by CD40. EMBO J. 2003; 22:3855–3864. [PubMed: 12881420]

4. Mielke LA, Elkins KL, Wei L, Starr R, Tsichlis PN, O'Shea J, Watford WT. Tumor progression locus 2 (Map3k8) is critical for host defense against Listeria monocytogenes and IL-1 production. J. Immunol. 2009; 183:7984–7993. [PubMed: 19933865]

5. Kontoyiannis D, Boulougouris G, Manoloukos M, Armaka M, Apostolaki M, Pizarro TT, Kotlyarov A, Forster I, Flavell RA, Gaestel M, Tsichlis PN, Cominelli F, Kollias G. Genetic dissection of the cellular pathways and signaling mechanisms in modeled tumor necrosis factor-induced Crohn's-like inflammatory bowel disease. J Exp Med. 2002; 196:1563–1574. [PubMed: 12486099]

6. George D, Salmeron A. Cot/TPL-2 protein kinase as a target for the treatment of inflammatory disease. Curr. Topics. Med. Chem. 2009; 9:611–622.

7. Watford WT, Wang C-C, Tsatsanis C, Mielke LA, Eliopoulos AG, Daskalakis C, Charles N, Odom S, Rivera J, O'Shea J, Tsichlis PN. Ablation of tumor progression locus 2 promotes a type 2 Th cell response in ovalbumin-immunized mice. J. Immunol. 2009; 184:105–113. [PubMed: 19955521]

8. Watford WT, Hissong BD, Durant LR, Yamane H, Muul LM, Kanno Y, Tato CM, Ramos HL, Berger AE, Mielke L, Pesu M, Solomon B, Frucht DM, Paul WE, Sher A, Jankovic D, Tsichlis PN, O'Shea JJ. Tpl2 kinase regulates T cell interferon-γ production and host resistance to Toxoplasma gondii. J. Exp. Med. 2008; 205:2803–2812. [PubMed: 19001140]

9. Glimcher LH, Murphy KM. Lineage commitment in the immune system: the T helper lymphocyte grows up. Genes Dev. 2000; 14:1693–1711. [PubMed: 10898785]

10. Korn T, Bettelli E, Oukka M, Kuchroo VK. IL-17 and Th17 cells. Annu. Rev. Immunol. 2009; 27:485–517. [PubMed: 19132915]

11. Becher B, Segal BM. Th17 cytokines in autoimmune neuro-inflammation. Curr Opin Immunol. 2011; 23:707–712. [PubMed: 21907555]

12. Krishnamoorthy G, Wekerle H. EAE: an immunologist's magic eye. Eur. J. Immunol. 2009; 39:1991–2058. [PubMed: 19672889]

13. Denic A, Johnson AJ, Bieber AJ, Warrington AE, Rodriguez M, Pirko I. The relevance of animal models in multiple sclerosis research. Pathophys. 2010; 18:21–29.

14. Papoutsopoulou S, Symons A, Tharmalingham T, Belich MP, Kaiser F, Kioussis D, O'Garra A, Tybulewicz V, Ley SC. ABIN-2 is required for optimal activation of the TPL-2/ERK MAP kinase pathway in innate immune responses. Nature Immunol. 2006; 7:606–615. [PubMed: 16633345]

15. Dann A, Poeck H, Croxford AL, Gaupp S, Kierdorf K, Knust M, Pfeifer D, Maihoefer C, Endres S, Kalinke U, Meuth SG, Wiendl H, Knobeloch KP, Akira S, Waisman A, Hartmann G, Prinz M. Cytosolic RIG-I-like helicases act as negative regulators of sterile inflammation in the CNS. Nat. Neurosci. 2011; 15:98–106. [PubMed: 22138643]

16. Sriskantharajah S, Belich MP, Papoutsopoulou S, Janzen J, Tybulewicz V, Seddon B, Ley SC. Proteolysis of NF-κB1 p105 is essential for T cell antigen receptor-induced proliferation. Nat. Immunol. 2009; 10:38–47. [PubMed: 19060899]

17. Boonstra A, Asselin-Paturel C, Gilliet M, Crain C, Trinchieri G, Liu YJ, O'Garra A. Flexibility of mouse classical and plasmacytoid-derived dendritic cells in directing T helper type 1 and 2 cell development: dependency on antigen dose and differential toll-like receptor ligation. J. Exp. Med. 2003; 197:101–109. [PubMed: 12515817]

18. Veldhoen M, Hirota K, Westendorft AM, Buer J, Dumoutier L, Renauld J-C, Stockinger B. The aryl hydrocarbon receptor links TH17-cell mediated autoimmunity to environmental toxins. Nature. 2008; 453:106–109. [PubMed: 18362914]

19. Veldhoen M, Hocking RJ, Atkins CJ, Locksley RM, Stockinger B. TGFβ in the context of an inflammatory cytokine milieu supports de novo differentiation of IL-17-producing cells. Immunity. 2006; 24:179–189. [PubMed: 16473830]

20. Kang Z, Altuntas CZ, Gulen MF, Liu C, Giltiay N, Qin H, Liu L, Qian W, Ransohoff RM, Bergmann C, Stohlman S, Tuohy VK, Li X. Astrocyte-restricted ablation of interleukin-17-induced Act1-mediated signaling ameliorates autoimmune encephalomyelitis. Immunity. 2010; 32:414–425. [PubMed: 20303295]

21. Chung Y, Chang SH, Martinez GJ, Yang XO, Nurieva R, Kang HS, Ma L, Watowich SS, Jetten AM, Tian Q, Dong C. Critical regulation of early TH17 cell differentiation by interleukin-1 signaling. Immunity. 2009; 30:576–587. [PubMed: 19362022]

22. Bettelli E, Korn T, Oukka M, Kuchroo VK. Induction and effector functions of TH17 cells. Nat. Rev. Immunol. 2008; 453:1051–1057.

23. Ivanov II, McKenzie BS, Zhou L, Tadokoro CE, Lepelley A, Lafaille JJ, Cua DJ, Littman DR. The orphan nuclear receptor RORγT directs the differentiation program of proinflammatory IL-17+ T helper cells. Cell. 2006; 126:1121–1133. [PubMed: 16990136]

24. Yang XO, Pappu BP, Nurieva R, Akimzhanov A, Kang HS, Chung Y, Ma L, Shah B, Panopoulos AD, Schluns KS, Watowich SS, Tian Q, Jetten AM, Dong C. T helper 17 lineage differentiation is programmed by orphan nuclear receptors ROR alpha and ROR gamma. Immunity. 2008; 28:29–39. [PubMed: 18164222]

25. McGeachy MJ, Anderton SM. Cytokines in the induction and resolution of experimental autoimmune encephalomyelitis. Cytokine. 2005; 32:81–84. [PubMed: 16153854]

26. Wilson EH, Weninger W, Hunter CA. Trafficking of immune cells in the central nervous system. J. Clin. Invest. 2010; 120:1368–1378. [PubMed: 20440079]

27. Kaiser F, Cook D, Papoutsopoulou S, Rajsbaum R, Wu X, Yang HT, Grant S, Ricciardi-Castagnoli P, Tsichlis PN, Ley SC, O'Garra A. TPL-2 negatively regulates interferon-beta production in macrophages and myeloid dendritic cells. J. Exp. Med. 2009; 206:1863–1871. [PubMed: 19667062]

28. Brereton CF, Sutton CE, Lalor SJ, Lavelle EC, Mills KHG. Inhibition of ERK MAPK suppresses IL-23- and IL-1-driven IL-17 production and attenuates autoimmune disease. J. Immunol. 2009; 183:1715–1723. [PubMed: 19570828]

29. Barr TA, Shen P, Brown S, Lampropoulou V, Roch T, Lawrie S, Fan B, O'Connor RA, Anderton SM, Bar-Or A, Fillatreau S, Gray D. B cell depletion therapy ameliorates autoimmune disease through ablation of IL-6-producing B cells. J. Exp. Med. 2012; 209:1001–1010. [PubMed: 22547654]

30. Matsushita T, Yanaba K, Bouaziz J-D, Fujimoto M, Tedder TF. Regulatory B cells inhibit EAE initiation in mice while other B cells promote disease progression. J. Clin. Invest. 2008; 118:3420–3420. [PubMed: 18802481]

31. Anderton SM, Fillatreau S. Activated B cells in autoimmune diseases: the case for a regulatory role. Nat. Clin. Pract. Rheumatol. 2008; 4:657–666. [PubMed: 19037227]

32. Fillatreau S, Sweenie MJ, McGeachy MJ, Gray D, Anderton SM. B cells regulate autoimmunity by provision of IL-10. Nat. Immunol. 2002; 3:944–950. [PubMed: 12244307]

33. Banerjee A, Gugasyan R, McMahon M, Gerondakis S. Diverse Toll-like receptors utilize Tpl2 to activate extracellular signal-regulated kinase (ERK) in hemopoietic cells. Proc Natl Acad Sci U S A. 2006; 103:3274–3279. [PubMed: 16484370]

34. Prendergast CT, Anderton SM. Immune cell entry to the central nervous system-current understanding and prospective therapeutic targets. Drug Targets. 2009; 9:315–327.

35. Reboldi A, Coisne C, Baumjohann D, Benvenuto F, Bottinelli D, Lira S, Uccelli A, Lanzavecchia A, Engelhardt B, Sallusto F. C-C chemokine receptor 6-regulated entry of Th17 cells into the CNS through the chorid plexus is required for the initiation of EAE. Nat. Immunol. 2009; 10:514–523. [PubMed: 19305396]

36. Zepp J, Wu L, Li X. IL-17 receptor signaling and T helper 17-mediated autoimmune demyelinating disease. Trends Immunol. 2011; 32:232–239. [PubMed: 21493143]

37. Heppner FL, Greter M, Marino D, Falsig J, Raivich G, Hovelmeyer N, Waisman A, Rulicke T, Prinz M, Priller J, Becher B, Aguzzi A. Experimental autoimmune encephalomyelitis repressed by micoglial paralysis. Nat. Med. 2005; 11:146–152. [PubMed: 15665833]

38. van Loo G, De Lorenzi R, Schmidt H, Huth M, Mildner A, Schmidt-Supprian M, Lassmann H, Prinz M, Pasparakis M. Inhibition of transcription factor NF-kB in the central nervous system ameliorates autoimmune encephalomyelitis in mice. Nat. Immunol. 2006; 7:954–961. [PubMed: 16892069]

39. Chastain EML, Duncan AS, Rodgers JM, Miller SD. The role of antigen presenting cells in multiple sclerosis. Biochim. Biophys. Acta. 2011; 1812:265–274. [PubMed: 20637861]

40. Wang X, Deckert M, Xuan NT, Nishanth G, Just S, Waisman A, Naumann M, Schluter D. Astrocytic A20 ameliorates experimental autoimmune encephalomyelitis by inhibiting NF-κB and STAT1-dependent. Acta Neuropathol. 2013 DOI 10.1007/s00401-013-1183-9.

41. Yang HT, Papoutsopoulou M, Belich M, Brender C, Janzen J, Gantke T, Handley M, Ley SC. Coordinate regulation of TPL-2 and NF-κB signaling in macrophages by NF-κB1 p105. Mol. Cell. Biol. 2012; 32:3438–3451. [PubMed: 22733995]

42. Lang V, Symons A, Watton SJ, Janzen J, Soneji Y, Beinke S, Howell S, Ley SC. ABIN-2 forms a ternary complex with TPL-2 and NF-κB1 p105 and is essential for TPL-2 protein stability. Mol. Cell. Biol. 2004; 24:5235–5248. [PubMed: 15169888]

43. Salmeron A, Ahmad TB, Carlile GW, Pappin D, Narsimhan RP, Ley SC. Activation of MEK-1 and SEK-1 by Tpl-2 proto-oncoprotein, a novel MAP kinase kinase kinase. EMBO J. 1996; 15:817–826. [PubMed: 8631303]

44. Prinz M, Schmidt H, Mildner A, Knobeloch K-P, Hanisch U-K, Raasch J, Merkler D, Detje C, Gutcher I, Mages J, Lang R, Martin R, Gold R, Becher B, Bruck W, Kalinke U. Distinct and nonredundant in vivo functions of IFNAR on myeloid cells limit autoimmunity in the central nervous system. Immunity. 2008; 28:675–686. [PubMed: 18424188]

45. Prinz M, Knobeloch K-P. Type I interferons as ambiguous modulators of chronic inflammation in the central nervous system. Frontiers Immunol. 2012; 3:1–9.

46. Kleinnijenhuis J, Oosting M, Joosten LAB, Netea MG, van Crevel R. innate immune recognition of Mycobacterium tuberculosis. Clin. Devel. Immunol. 2011 In press.

47. Marta M. Toll-like receptors in multiple sclerosis mouse experimental models. Ann. N.Y. Acad. Sci. 2009; 1173:458–462. [PubMed: 19758186]

48. Prinz M, Priller J, Sisodia SS, Ransohoff RM. Heterogeneity of CNS myeloid cells and their roles in neurodegeneration. Nat. Neurosci. 2011; 14:1227–1235. [PubMed: 21952260]

49. Goldmann T, Wieghofer P, Muller PF, Wolf Y, Varol D, Yona S, Brendecke SM, Kierdorf K, Staszewski O, Datta M, Luedde T, Heikenwalder M, Jung S, Prinz M. A new type of microglia gene targeting shows TAK1 to be pivotal in CNS autoimmune inflammation. Nat. Neurosci. 2013; 16 doi:10.1038/nn.3531.

50. Beinke S, Robinson MJ, Salmeron A, Hugunin M, Allen H, Ley SC. Lipopolysaccharide activation of the TPL-2/MEK/Extracellular signal-regulated kinase mitogen-activated protein kinase cascade is regulated by IκB kinase-induced proteolysis of NF-κB1 p105. Mol. Cell. Biol. 2004; 24:9658–9667. [PubMed: 15485931]

51. Waterfield M, Jin W, Reiley W, Zhang MY, Sun S-C. IKKβ is an essential component of the TPL-2 signaling pathway. Mol. Cell Biol. 2004; 24:6040–6048. [PubMed: 15199157]

52. Roget K, Ben-Addi A, Mambole-Dema A, Gantke T, Janzen J, Yang H-T, Shpiro N, Morrice N, Abbott D, Ley SC. IKK2 regulates TPL-2 activation of ERK-1/2 MAP kinases by direct phosphorylation of TPL-2 serine 400. Mol. Cell. Biol. 2012; 32:4684–4690. [PubMed: 22988300]

53. Consortium, I. M. S. G.; W. T. C. C. C. 2. Genetic risk and a primary role for cell-mediated immune mechanisms in multiple sclerosis. Nature. 2011; 476:214–219. [PubMed: 21833088]
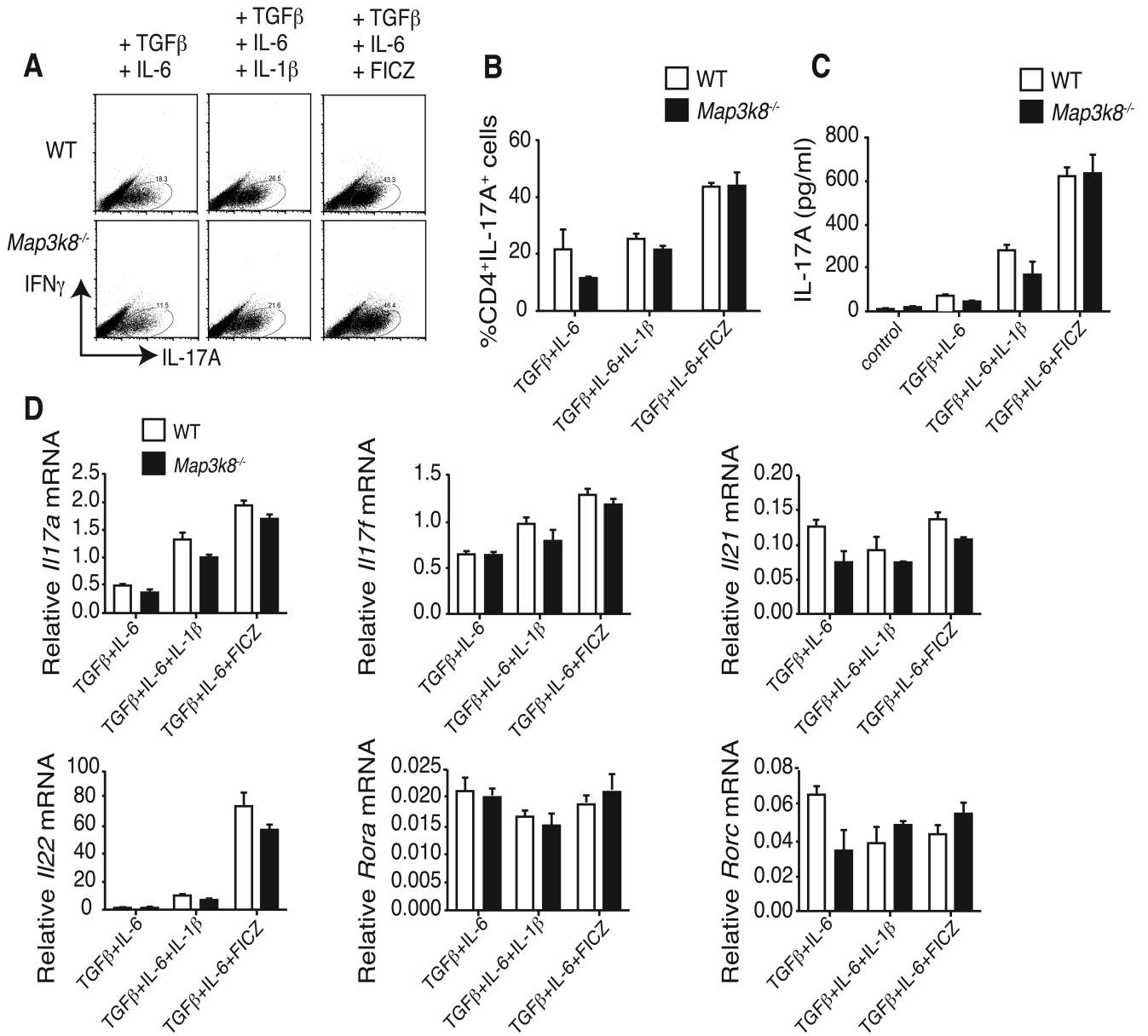
Figure 1. TPL-2 is not required for *in vitro* differentiation of Th17 cells
(A - C) CD25⁻ CD44hiCD4⁺ T cells (naïve CD4⁺ T cells) were isolated from WT (*Map3k8*⁺/⁺) and *Map3k8*⁻/⁻ mice by FACS sorting, and cultured in triplicates for 4 days with anti-CD3/anti-CD28 plus the indicated Th17 polarizing cytokines and the AhR ligand FICZ. (A and B) IFNγ and IL-17A expression in CD4⁺ T cells was determined by intracellular staining and flow cytometry (mean ± s.e.m.). (C) ELISA of IL-17A production by CD4⁺ T cells (mean + s.e.m.). (D) Expression of the indicated mRNAs in Th17-polarized cell populations was determined by qRT-PCR, presented relative to *Hprt1* mRNA (mean ± s.e.m.). Data are representative for three independent experiments.
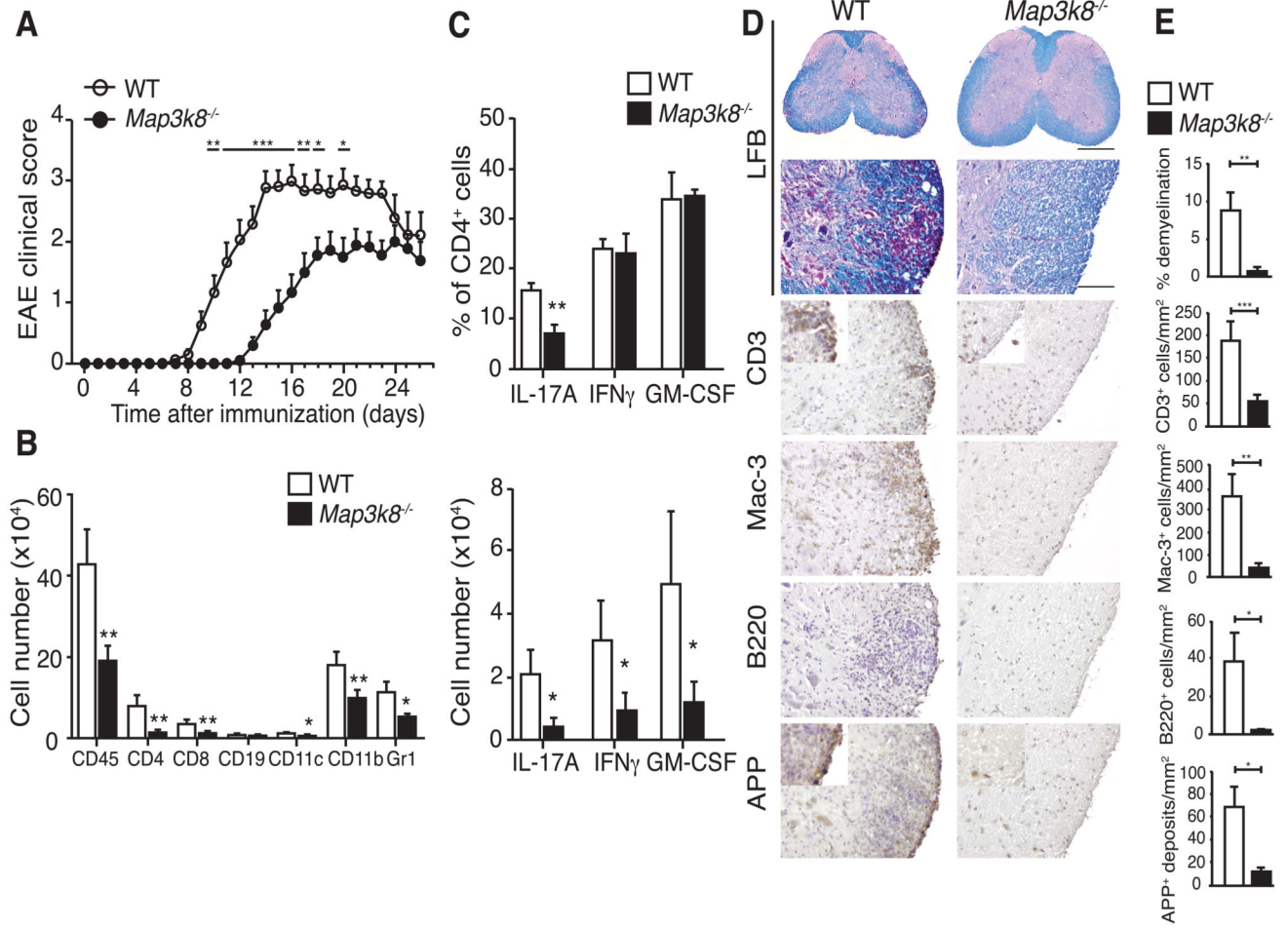
Figure 2. TPL-2 regulates the onset and severity of EAE

(A) Mean clinical scores of WT and $Map3k8^{-/-}$ mice (n = 19/WT; n=18/$Map3k8^{-/-}$) at various times after immunization with MOG_{33-55}/CFA. Data presented are combined from two independent experiments (n = 9-10/genotype/experiment). (B) Immune cell infiltration in the spinal cords of WT and $Map3k8^{-/-}$ mice (n = 8/genotype) at the peak of disease was determined by flow cytometry using the indicated markers (mean ± s.e.m.) (C) Intracellular staining for infiltrated IL-17A-, IFNγ– and GM-CSF-expressing $CD4^+$ T cells in the spinal cords of WT and $Map3k8^{-/-}$ mice (n=8/genotype) on d12 after MOG_{33-55}/CFA immunization. In D and E, EAE was induced in WT and $Map3k8^{-/-}$ mice, and spinal cords removed at the peak of disease. (D) Spinal cord sections were stained with luxol fast blue (LFB) to monitor demyelination (scale bar represents 200μm in the first panel, and 50μm in the lower panels). Immune cell infiltration was revealed by antibody staining: CD3 for T cells, Mac-3 for macrophages and B220 for B cells. Axonal damage was visualized by staining for amyloid precursor protein (APP). (E) Quantitation of demyelination, immune infiltration and axonal damage (mean ± s.e.m.). Data in B and C are compiled from 2 independent experiments (n=4/genotype/experiment). Data in D and E are representative of two independent experiments. * p   0.05; ** p 0.01; *** p 0.001.
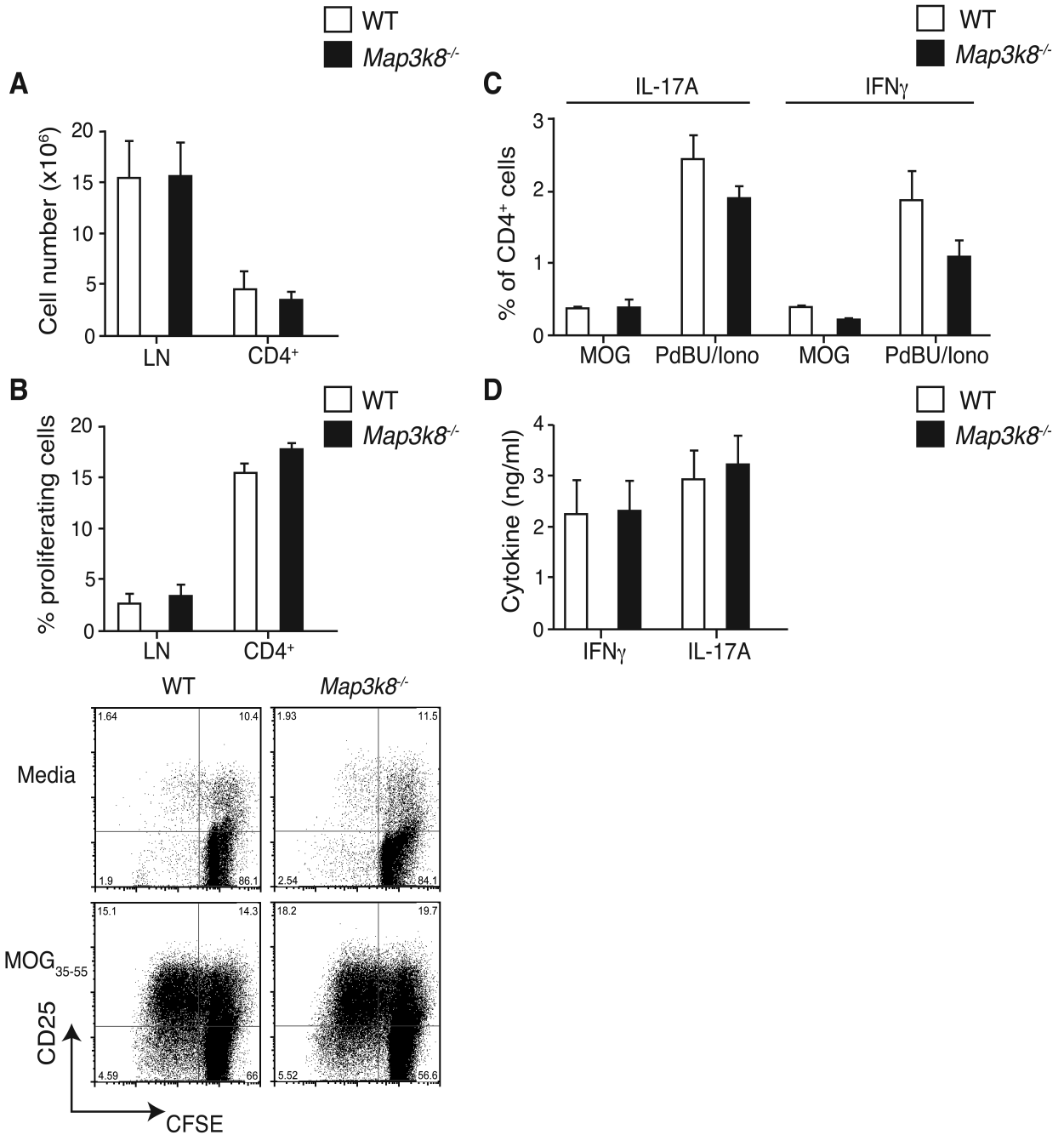
Figure 3. TPL-2 is not required for T cell priming in EAE
WT and *Map3k8*$^{-/-}$ mice were immunized with MOG$_{33-55}$/CFA, and draining LN isolated on d9. (A) CD4$^+$ T cell numbers were determined by flow cytometry (mean ± s.e.m.; n = 3). (B) Flow cytometric analysis of the proliferation of CFSE-labelled CD4$^+$ T cells cultured for 3d with MOG$_{33-55}$ peptide (mean ± s.e.m.; n = 3). (C) Frequencies of IL-17A- and IFNγ–expressing CD4$^+$ T cells were determined by flow cytometry, after restimulation with PdBu/ionomycin or MOG$_{33-55}$ peptide (mean ± s.e.m.; n = 3). (D) ELISA of IFNγ and IL-17A production by LN cells restimulated with MOG$_{33-55}$ peptide (mean ± s.e.m.; n = 3). Data are representative of at least three independent experiments.
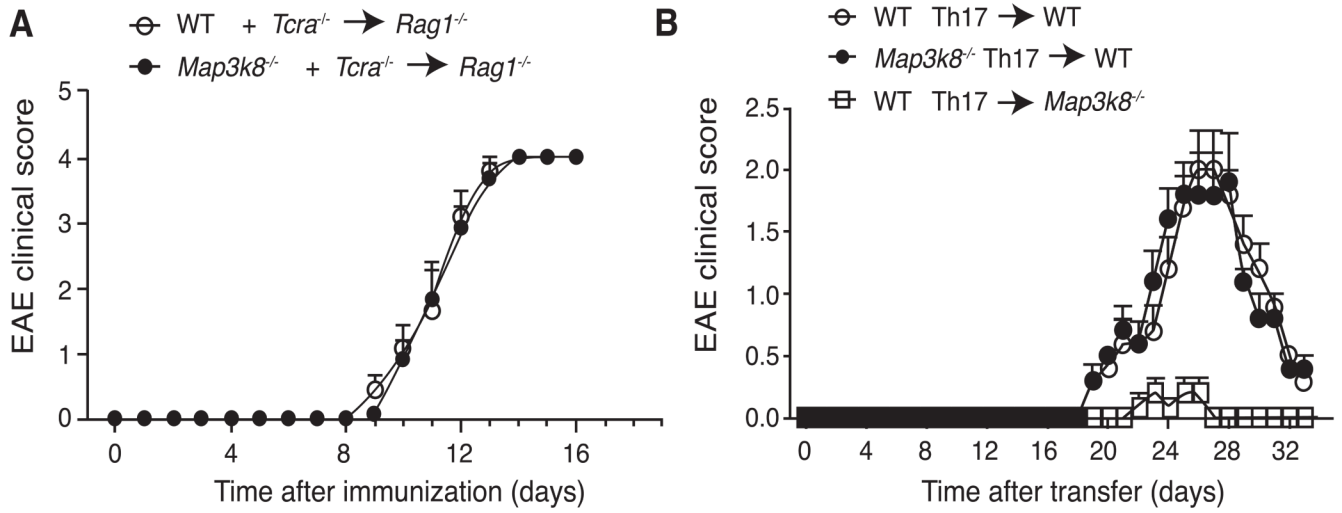
Figure 4. TPL-2 signaling in T cells is not required for EAE development
(A) BM cells from WT and *Map3k8*$^{-/-}$ mice were mixed in a 1:4 ratio with BM cells from *Tcra*$^{-/-}$ mice, and transferred into *Rag1*$^{-/-}$ hosts. After 8 weeks, EAE was induced by immunization with MOG$_{33-55}$/CFA, and clinical scores determined (mean ± s.e.m.; n = 6). (B) Draining LN cells from WT and *Map3k8*$^{-/-}$ mice were isolated 9d after immunization with MOG$_{33-55}$/CFA, and restimulated *in vitro* with MOG$_{33-55}$ peptide in the presence of recombinant IL-1β and 1L-23 for 5d. These Th17-polarized cells were then transferred into naïve WT and *Map3k8*$^{-/-}$ mice. Graph represents the average clinical score after Th17 cell transfer (mean ± s.e.m.; n = 5). Data in A and B are representative of two independent experiments.
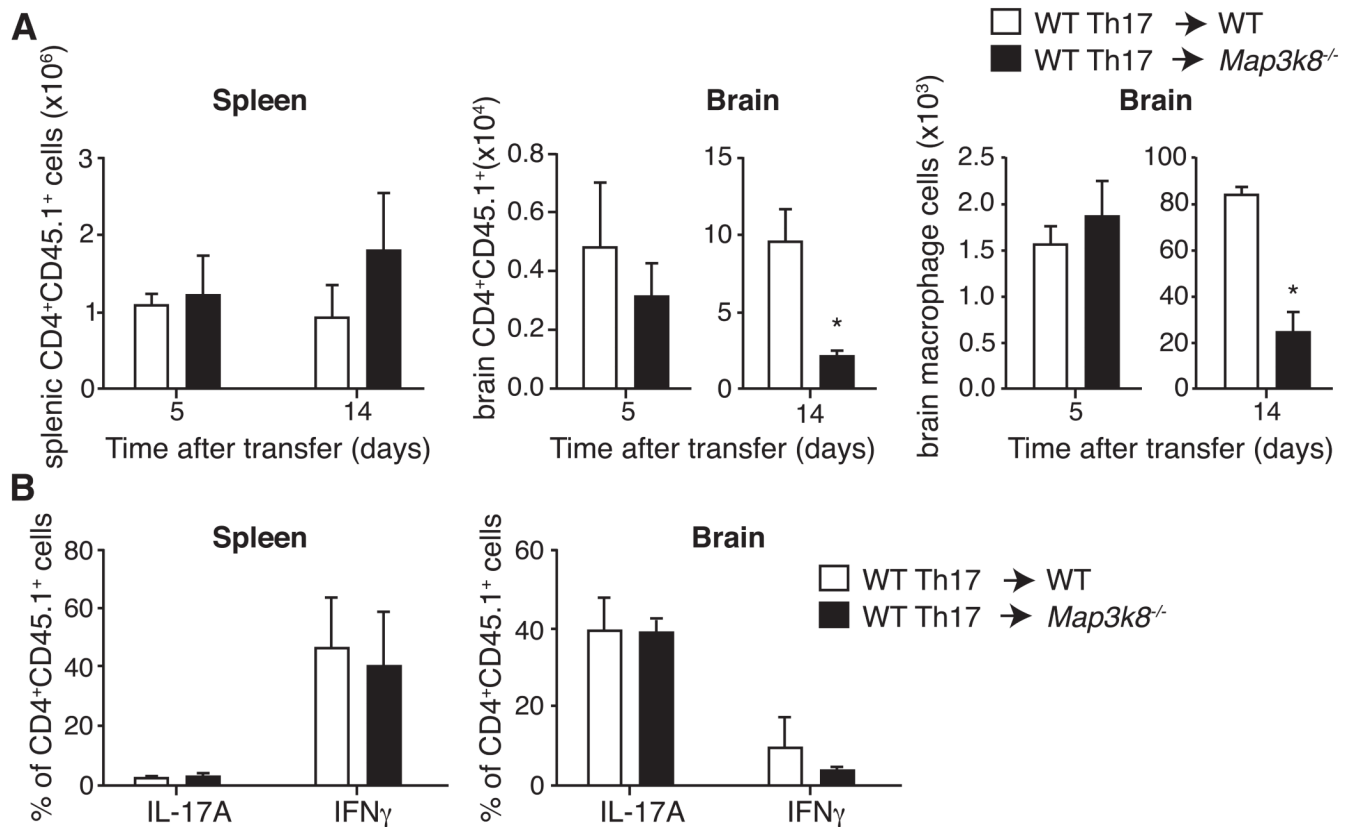
Figure 5. TPL-2 regulates the effector phase of EAE
(A) MOG$_{33-55}$-specific Th17 cells were generated from CD45.1$^+$ WT mice, and then transferred into CD45.2$^+$ WT and *Map3k8*$^{-/-}$ mice as in Figure 6C. Numbers of CD45.1$^+$ CD4$^+$ T cells in the spleen and brain were determined by flow cytometry at the indicated time points after Th17 cell transfer (mean ± s.e.m.; n = 3). Macrophage numbers in the brain after transfer were determined by F4/80 staining. (B) Intracellular staining for IL-17A- and IFNγ-expression in transferred Th17 polarized CD45.1$^+$ CD4$^+$ T cells in the spleen and brain on d14 after transfer (mean ± s.e.m., n=3). Data are representative of at least two independent experiments. * p   0.05
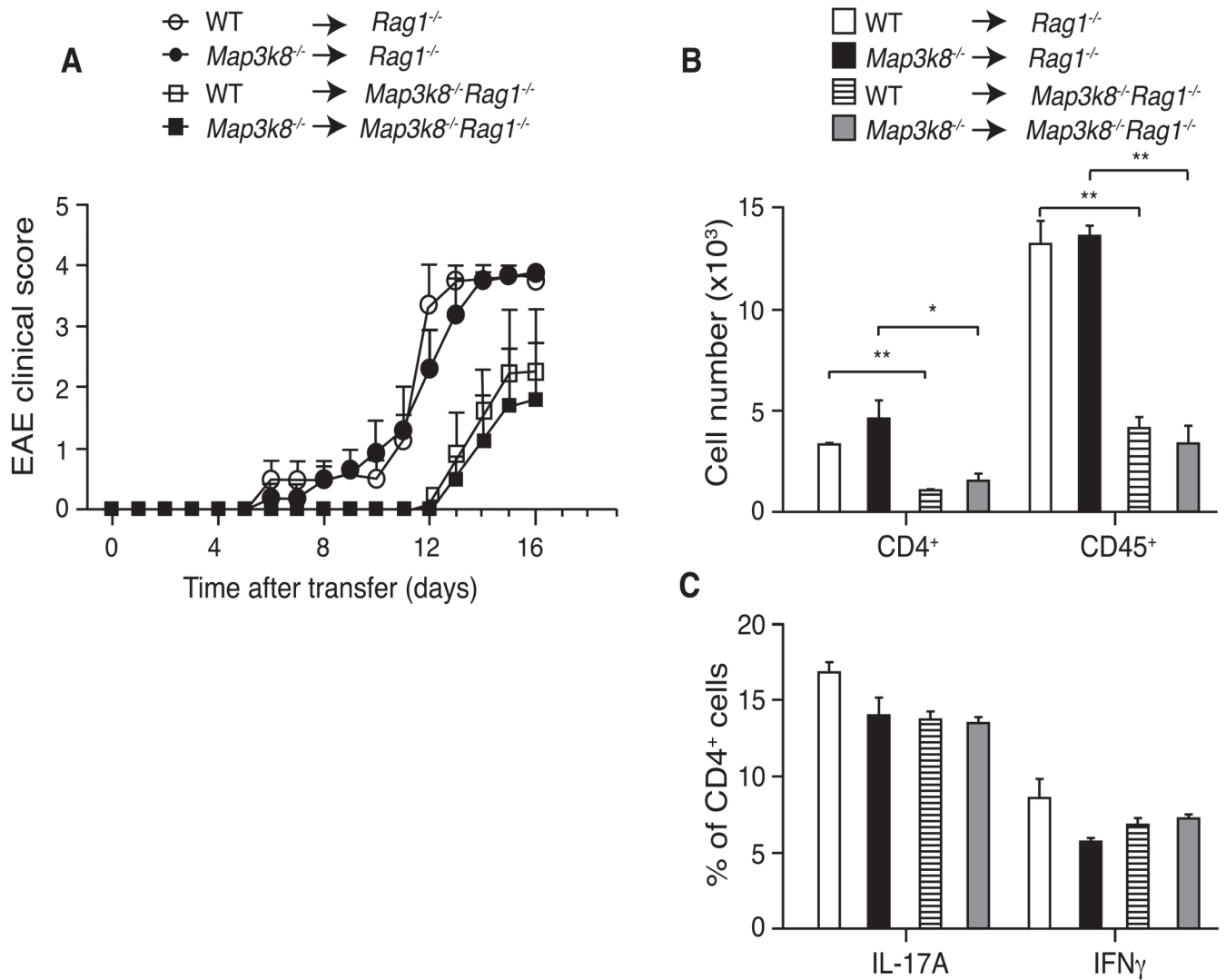
Figure 6. TPL-2 signaling in radiation-resistant cells promotes EAE
(A) BM cells from WT and $Map3k8^{-/-}$ mice were adoptively transferred into lethally irradiated $Rag1^{-/-}$ or $Map3k8^{-/-}Rag1^{-/-}$ hosts, and EAE induced 8 weeks later. Mean clinical scores are shown (mean ± s.e.m; n = 4-5). (B and C) EAE was induced in chimeric mice generated as in A. (B) Total numbers of $CD4^+$ and $CD45^+$ cells in the spinal cords 12d after MOG_{33-55} peptide plus CFA immunization were determined by flow cytometry (mean ± s.e.m., n=4). (C) Intracellular staining for IL-17A- and IFNγ–expressing $CD4^+$ T cells in the spinal cord at peak of disease (mean ± s.e.m.; n = 4). Data are representative for three independent experiments. * p 0.05; ** p 0.01.
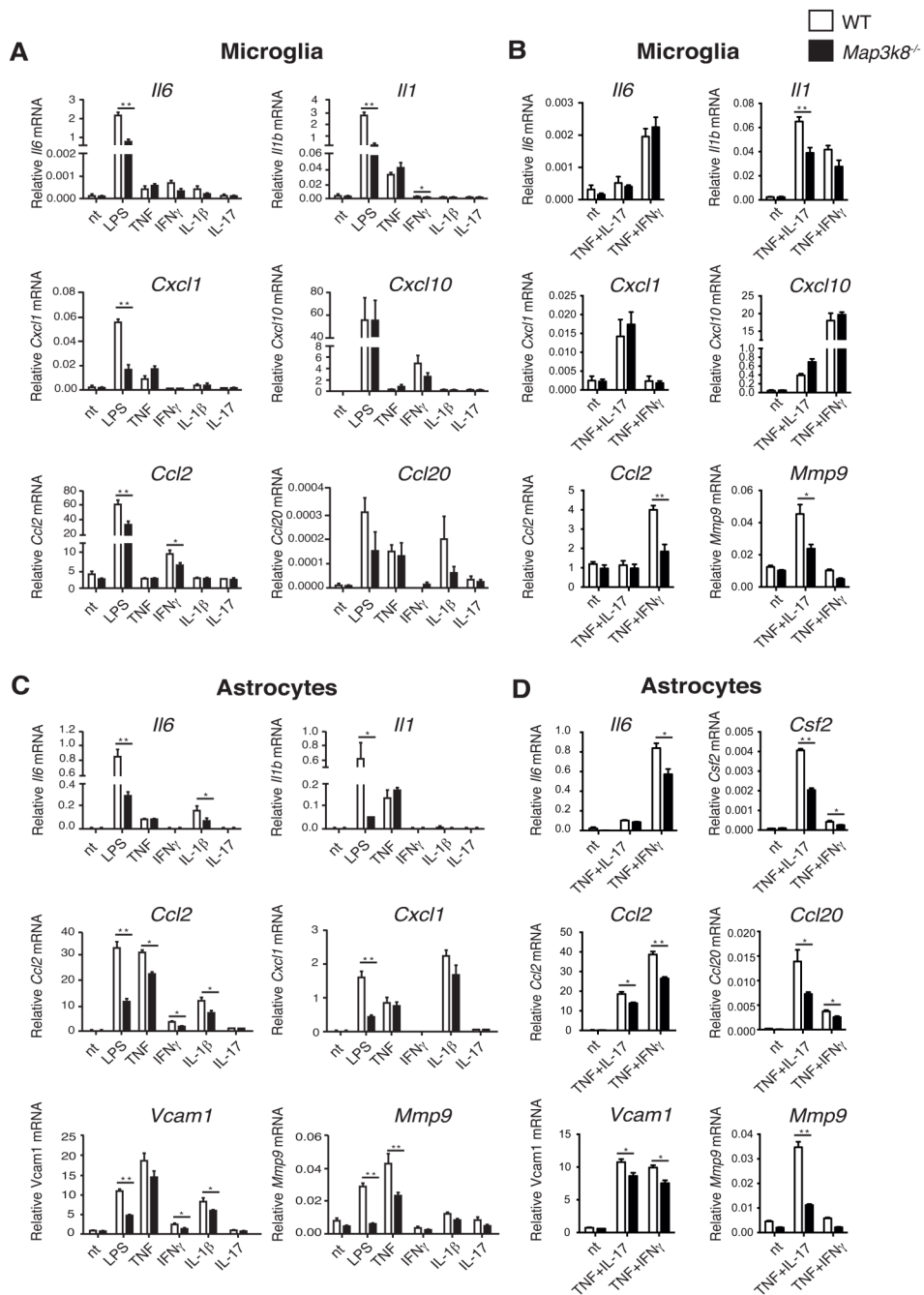
Figure 7. TPL-2 regulates pro-inflammatory gene expression in primary microglia and astrocytes

Quantitative RT-PCR of mRNA expression in primary microglia (A, B) and astrocytes (C, D) from WT and *Map3k8*$^{-/-}$ mice, normalized to *Hprt* mRNA (mean ± s.e.m.). Cells were either left untreated (nt) or stimulated with the indicated agonists for 6h. Data are compiled from three (A, C) or two (B, D) independent experiments. * p 0.05, ** p 0.01.
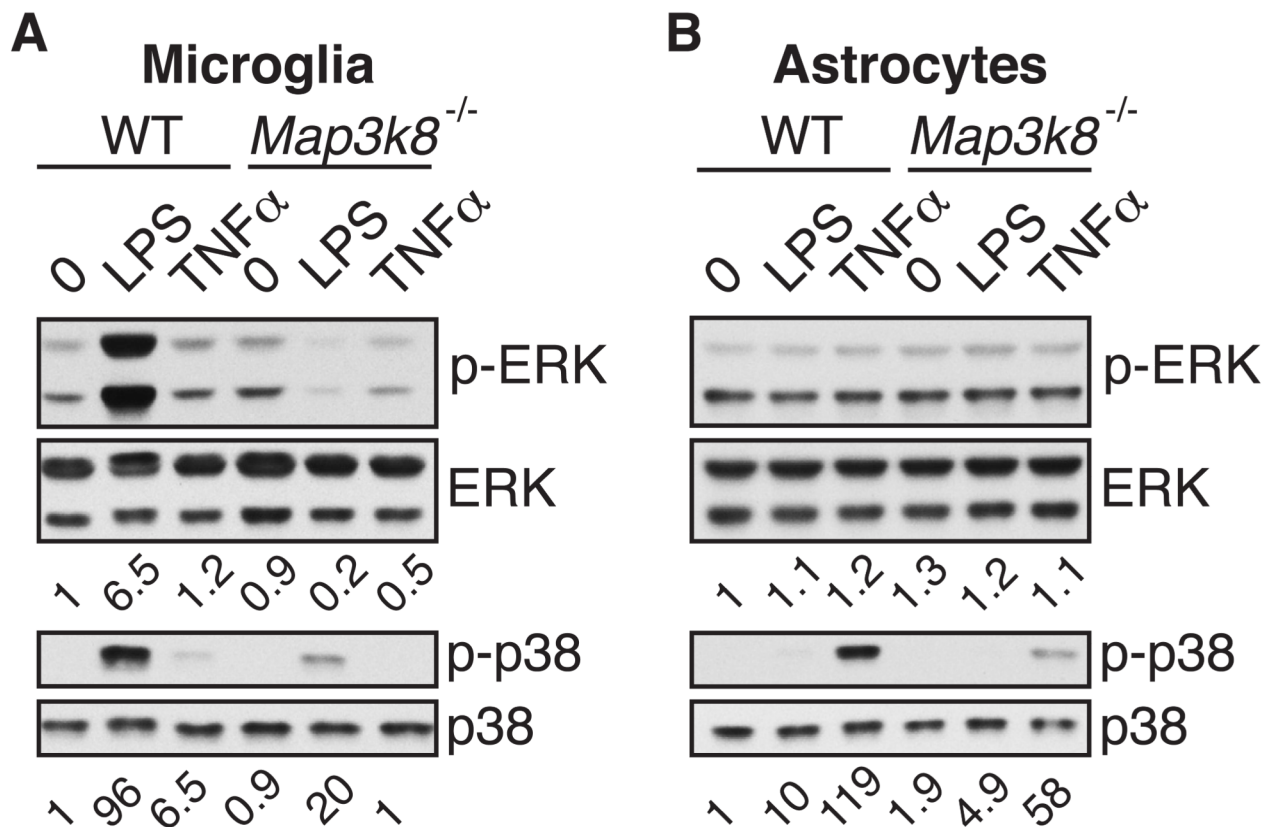
Figure 8. TPL-2 is required for optimal MAP kinase activation in microglia and astrocytes
Lysates of microglia (A) and astrocytes (B), generated from WT and *Map3k8*$^{-/-}$ mice and stimulated for the indicated time points with LPS or TNF, were immunoblotted. Phosphorylated protein bands were quantified by laser densitometry using the Quantity One software package, and are presented as relative density normalized to the respective total protein. Data are representative for 3 – 4 independent experiments with similar results.
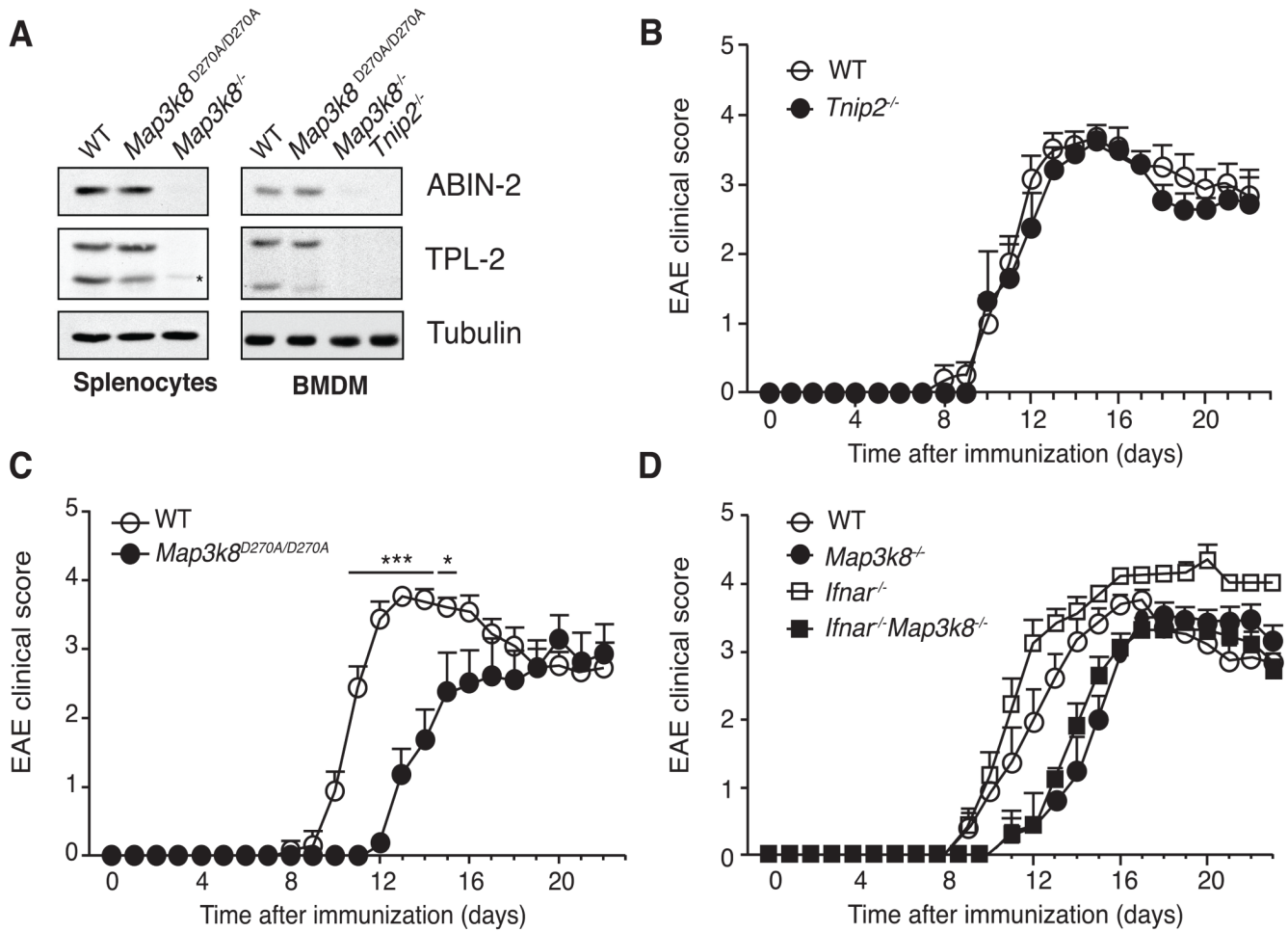
Figure 9. TPL-2 kinase activity is required to induce EAE
(A) Lysates were prepared from splenocytes (left panel) and BMDM (right panel) generated from WT, $Map3k8^{-/-}$, $Map3k8^{D270A/D270A}$ and $TNIP2^{-/-}$ mice, and immunoblotted for the indicated antigens. (B) Mean clinical scores of WT and $Tnip2^{-/-}$ mice (mean ± s.e.m.; n = 7 - 8). Data are compiled from 2 different experiments (n = 3-4/genotype/experiment). (C) Mean clinical scores of WT, $Map3k8^{D270A/D270A}$ and $Map3k8^{-/-}$ mice mice at various times after immunization with MOG_{33-55}/CFA (mean ± s.e.m.; n = 8 - 9). Data are compiled from 2 different experiments (n = 3-4/genotype/experiment). * p 0.05; *** p 0.001. (D) Mean clinical scores of WT, $Map3k8^{-/-}$, $Ifnar^{-/-}$ and $Map3k8^{-/-}Ifnar^{-/-}$ mice after immunization with MOG_{33-55}/CFA (mean ± s.e.m.; n = 9 - 10). Data are compiled from 2 different experiments (n = 4-5/genotype/experiment).

Table 1

Clinical features of MOG$_{35\text{-}55}$–induced EAE

	Incidence	Mean maximum score (Mean ± S.D.)	Mean day of onset (Mean ± S.D.)
WT	19/19 (100%)	3.5 ± 0.9	10.52 ± 2.1
Map3k8$^{-/-}$	18/18 (100%)	2.7 ± 0.9	15.07 ± 2.5